PHILOSOPHICAL TRANSACTIONS OF THE ROYAL SOCIETY B

Phil. Trans. R. Soc. B (2010) **365**, 3377–3388
doi:10.1098/rstb.2010.0042

Hominin diversity in the Middle Pliocene of eastern Africa: the maxilla of KNM-WT 40000

Fred Spoor[1,2,*], **Meave G. Leakey**[3,4] **and Louise N. Leakey**[3,5]

[1]*Department of Human Evolution, Max Planck Institute for Evolutionary Anthropology, Deutscher Platz 6, 04103 Leipzig, Germany*
[2]*Department of Cell and Developmental Biology, University College London, UK*
[3]*Koobi Fora Research Project, Nairobi, Kenya*
[4]*Department of Anatomical Sciences, and*
[5]*Department of Anthropology, Stony Brook University, New York, USA*

The 3.5-Myr-old hominin cranium KNM-WT 40000 from Lomekwi, west of Lake Turkana, has been assigned to a new hominin genus and species, *Kenyanthropus platyops*, on the basis of a unique combination of derived facial and primitive neurocranial features. Central to the diagnosis of *K. platyops* is the morphology of the maxilla, characterized by a flat and relatively orthognathic subnasal region, anteriorly placed zygomatic processes and small molars. To study this morphology in more detail, we compare the maxillae of African Plio-Pleistocene hominin fossils and samples of modern humans, chimpanzees and gorillas, using conventional and geometric morphometric methods. Computed tomography scans and detailed preparation of the KNM-WT 40000 maxilla enable comprehensive assessment of post-mortem changes, so that landmark data characterizing the morphology can be corrected for distortion. Based on a substantially larger comparative sample than previously available, the results of statistical analyses show that KNM-WT 40000 is indeed significantly different from and falls outside the known range of variation of species of *Australopithecus* and *Paranthropus*, contemporary *Australopithecus afarensis* in particular. These results support the attribution of KNM-WT 40000 to a separate species and the notion that hominin taxonomic diversity in Africa extends back well into the Middle Pliocene.

Keywords: human evolution; Pliocene; Africa; *Kenyanthropus platyops*; maxilla; geometric morphometrics

1. INTRODUCTION

Whether or not the Pliocene hominin fossil record from Hadar (Ethiopia) and Laetoli (Tanzania) represents more than one species was the subject of ongoing debate in the 1980s (see Boaz 1988 for a review). Recovery of additional fossils and studies of intraspecific variation and temporal trends have subsequently resulted in a broad consensus supporting the interpretation of a single, sexually dimorphic species, *Australopithecus afarensis* (Lockwood *et al.* 1996, 2000; Kimbel *et al.* 2004; Kimbel & Delezene 2009). However, fossils found at two other sites have reopened the debate of species diversity in the African Middle Pliocene. A partial mandible and upper premolar, discovered in 1994 in the Koro-Toro area of Chad and approximately 3.5 Myr old, have been assigned to a new species, *Australopithecus bahrelghazali* (Brunet *et al.* 1995, 1996). This attribution has been questioned as the limited morphology preserved by these fossils is considered to be within the range of variation of *A. afarensis* (White *et al.* 2000; Ward *et al.* 2001; Kimbel 2007; Wood & Lonergan 2008). However, a detailed analysis of symphyseal shape of both the type specimen and a previously unpublished second mandible supports a separate specific status (Guy *et al.* 2008).

A second site providing possible evidence for species diversity is Lomekwi, west of Lake Turkana (Kenya). Fieldwork in the early 1980s and late 1990s resulted in hominin discoveries dated between 3.5 and 3.2 Ma, including a well-preserved temporal bone, 2 partial maxillae, 3 partial mandibles, 44 isolated teeth and a largely complete although distorted cranium, KNM-WT 40000 (Brown *et al.* 2001; Leakey *et al.* 2001). Several of these specimens were found to show a morphology markedly different from that of contemporary *A. afarensis* (Leakey *et al.* 2001). Accordingly, the cranium and one fragmentary maxilla were assigned to a new genus and species, *Kenyanthropus platyops*, based on a unique combination of derived facial and primitive neurocranial features (Leakey *et al.* 2001). A number of recent studies and reviews have cautiously considered *K. platyops* as a valid taxon (Strait & Grine 2004; Kimbel 2007; Cobb 2008; Nevell & Wood 2008;

* Author for correspondence (f.spoor@eva.mpg.de).

Electronic supplementary material is available at http://dx.doi.org/10.1098/rstb.2010.0042 or via http://rstb.royalsocietypublishing.org.

One contribution of 14 to a Discussion Meeting Issue 'The first four million years of human evolution'.

This journal is © 2010 The Royal Society

Wood & Lonergan 2008). On the other hand, White (2003) questioned the taxon's validity, and the notion of Pliocene hominin diversity. In his view it cannot be excluded that KNM-WT 40000 is an early Kenyan variant of *A. afarensis*, given the distortion of the specimen and the known cranial variation in early hominin species and among modern apes and humans.

Central to the diagnosis of *K. platyops* is the morphology of the maxilla, characterized by a flat and relatively orthognathic subnasal region, an anteriorly placed zygomatic process and small molars. In the present study, this morphology, as shown by KNM-WT 40000, is investigated in more detail. We made quantitative comparisons, using geometric morphometric and univariate methods, with Plio-Pleistocene hominin fossils from Ethiopia, Kenya, Tanzania and South Africa and with samples of modern humans, gorillas and chimpanzees. Such analyses are obviously affected by the post-mortem distortion of KNM-WT 40000, the reason the initial description provided limited metric comparisons only (Leakey *et al.* 2001). The impact of the preservation of the maxilla was therefore evaluated in detail using new evidence based on additional preparation of the specimen and computed tomography (CT). The information thus obtained was used to adjust landmarks representing the key morphological features. In statistical analyses the morphology of the specimen is considered both in its preserved form and corrected for distortion.

Using a substantially larger comparative sample than available to Leakey *et al.* (2001), the present study aims to assess two specific hypotheses.

1. KNM-WT 40000 does not differ significantly from *A. afarensis* with respect to the morphological features of the maxilla included in the differential diagnosis of *K. platyops* (Leakey *et al.* 2001). Rejection of this null hypothesis would provide evidence for species diversity in eastern Africa at around 3.5 Ma.
2. KNM-WT 40000 does not differ significantly from species of *Australopithecus* and *Paranthropus* with respect to the morphological features of the maxilla included in the differential diagnosis of *K. platyops* (Leakey et al. 2001). Rejection of this null hypothesis would support the attribution of KNM-WT 40000 to a separate species.

2. MATERIAL AND METHODS

In geometric morphometric shape analyses the KNM-WT 40000 maxilla was compared with all available hominin specimens attributed to *Australopithecus* and *Paranthropus* that preserve the morphology concerned. These are: *Australopithecus anamensis* (KNM-KP 29283), *A. afarensis* (A.L. 199-1, A.L. 200-1, A.L. 417-1, A.L. 427-1, A.L. 444-2 and A.L. 486-1), *Australopithecus africanus* (MLD 9, Sts 52, Sts 71 and Stw 498), *Australopithecus garhi* (BOU-VP-12/130), *Paranthropus aethiopicus* (KNM-WT 17000), *Paranthropus boisei* (OH 5) and *Paranthropus robustus* (SK 11, SK 12, SK 13, SK 46, SK 48, SK 83 and SKW 11). All are adults, with the exception of A.L. 486-1, Sts 52, OH 5, SK 13 and SKW 11, which are subadults (third molars not in occlusion).

The intraspecific variation in maxillary shape among the fossils was examined by making comparisons with samples of modern humans and African great apes. The modern human sample consists of 55 specimens (sex mostly unknown), representing indigenous populations from all six widely inhabited continents, housed at the Natural History Museum (London) and at the Department of Cell and Developmental Biology at University College London. The African ape samples (all non-captive) include 50 specimens of the eastern lowland gorilla (*Gorilla gorilla gorilla*; 26 males, 24 females) and 61 specimens of chimpanzee (*Pan troglodytes*, all subspecies represented; 28 males, 33 females) from the collections of the Powell Cotton Museum (Birchington), the Royal College of Surgeons (London), the Natural History Museum (London) and the Department of Cell and Developmental Biology at University College London. Specimens are adult and lack signs of substantial pathology, of the alveolar process of the maxilla in particular.

CT was used to examine internal morphology and record surface landmarks of some of the fossil specimens. KNM-WT 40000 was scanned with a Siemens AR.SP medical scanner at the Diagnostic Center, Nairobi (Kenya). Scans in sequential mode were made in the transverse plane, parallel to the postcanine alveolar margin, using a slice thickness and increment of 1.0 mm. Images were reconstructed with a SP90 kernel, extended CT-scale and a 0.17 mm pixel size. The tooth roots were segmented by Kornelius Kupczik and the first author. New CT data with improved spatial resolution (isotropic voxel size 0.069 mm) were obtained more recently with the portable BIR ACTIS 225/300 high-resolution industrial CT scanner of the Department of Human Evolution at the Max Planck Institute for Evolutionary Anthropology (Leipzig, Germany), at the time installed at the National Museums of Kenya in Nairobi. Other CT data of hominin fossils used here are from the digital archives of the National Museums of Kenya, and the Department of Anthropology, University of Vienna. Visualization of the CT datasets was done using Amira 4.1.2 (Mercury Computer Systems).

A set of maxillary landmarks was selected using three criteria: (i) they should quantify the features used in the differential diagnosis of *K. platyops*; (ii) it should be possible to take these landmarks from the KNM-WT 40000 maxilla and correct them for distortion of the specimen; and (iii) the number of fossil specimens used in the comparative sample should be as large as possible. Optimizing all three criteria resulted in the selection of five two-dimensional landmarks, taken from the specimens projected in lateral view: nasospinale (ns), prosthion (pr), the buccal alveolar margin between the canine and third premolar (pc), the buccal alveolar margin between the second and third molar (m23) and the antero-inferior take-off of the zygomatic process (azp), a point most anterior, inferior and medial on the root of the process (figure 1). These landmarks quantify the orientation of

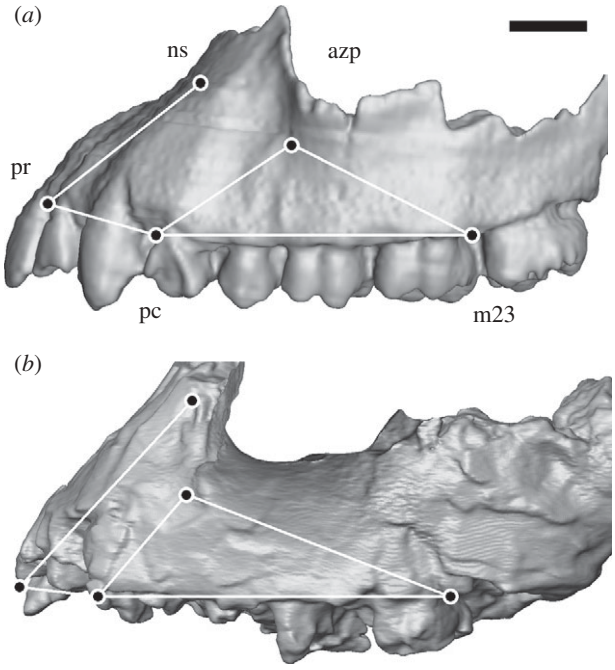

Figure 1. CT-based parallel-projected 3D reconstructions comparing the maxillae in lateral view of (*a*) A.L. 200-1 (reversed right side of cast, *Australopithecus afarensis*) and (*b*) KNM-WT 40000 (left side of original, *Kenyanthropus platyops*). The five landmarks are shown, together with the connecting wire frame used in figure 3 (see text for the abbreviations of the landmarks). The broken surface of the zygomatic process of KNM-WT 40000 facing laterally is not visualized to emphasize the outline compared with the equivalent morphology in A.L. 200-1. Scale bar, 10 mm.

the subnasal clivus in the midsagittal plane (ns-pr), the anterior zygomatic process position along the postcanine tooth row (azp relative to pc-m23) and the degree of anterior projection and transverse flatness of the subnasal clivus (pr–pc or sagittally projected length of the canine and incisor alveolar margin).

The five landmarks were mostly recorded from digital images of the specimens in exact lateral view and taken with a focal distance of 1–2 m to minimize parallax artefacts. Nasospinale and prosthion may not be visible in this view and are indicated by markers (see Spoor *et al.* 2005 for details of this method). The landmarks of KNM-WT 40000, A.L. 444-2, Sts 52a, Sts 71, KNM-WT 17000 and OH 5 were taken from CT datasets, using Amira 4.1.2 (Mercury Computer Systems) to obtain parallel-projected three dimensional surface reconstructions in a lateral view and sagittal sections to locate nasospinale and prosthion. The left side of the extant specimens was used, the mean of both sides of A.L. 200-1 and OH 5 and the best preserved side of the other fossils (left for KNM-WT 40000). All landmark coordinates were recorded with ImageJ 1.42d (National Institutes of Health, USA).

To examine the impact of the distortion of KNM-WT 40000 on the landmark positions, additional surface preparation was done of the anterior and lateral aspects of the left maxilla. Small remnants of the matrix on the bone surface were removed and cracks fully exposed. Bone edges on either side of the crack could thus be matched, identifying possible shifts along the crack. Moreover, the width of the cracks along specific trajectories linking the five landmarks (figure 2*a*,*d*) were measured to the nearest tenth of a millimetre with digital callipers, making sure that the distance was taken between matching edges. The midsagittal surface area above prosthion is not well preserved, and the expansion of the subnasal clivus in the sagittal plane was examined more laterally along a line from the I^2/C interalveolar septum to the left lower corner of the nasal aperture (figure 2*a*). The crack widths were used to calculate the percentage of surface expansion between the five landmarks, and the *x* and *y* coordinates were adjusted accordingly. Both preparation and measurements were done under a binocular microscope, using acetone to temporarily enhance the difference between bone and matrix.

Generalized procrustes analyses of the landmark coordinates and principal component analyses (PCAs) of the output were performed with Morphologika 2.5 (O'Higgins & Jones 1998). With this software, the maxillary shape variation associated with each principal component (PC) can be explored visually by morphing a wireframe of the five landmarks according to the position on a bivariate plot of two PCs. *F*-tests and *t*-tests of the individual PC scores, with sequential Bonferroni correction for multiplicity (Rice 1989), were done using PAST 1.93 (Hammer *et al.* 2001) and MS Excel 2003. One-tailed distributions were used in the *t*-tests when the hypotheses and the species diagnosis of *K. platyops* specifically state the nature of a possible difference (e.g. KNM-WT 40000 is subnasally less prognathic than *A. afarensis*). Consequently, two-tailed distributions were used only for the comparison of PCs related to zygomatic process position in KNM-WT 40000 and *P. robustus*, where there is no prior prediction of the nature of the difference. KNM-WT 40000 was also compared with species individually by combining all PCs obtained in separate analyses of KNM-WT 40000 and each species. The Mahalanobis' distance of KNM-WT 40000 from the centroid of the species sample is compared with the distances from that centroid of the specimens in the sample (software written by Paul O'Higgins, Hull York Medical School, UK). All statistical analyses were done separately for KNM-WT 40000 in its preserved form and corrected for distortion.

A drawback of the landmark-based approach is that it limits the number of specimens that can be included. That is because each must preserve the full area covered by the landmarks, whereas less complete specimens may be informative regarding individual diagnostic aspects of the *K. platyops* maxilla. When interpreting the main shape analysis, two maxillary features were therefore considered individually as well, to assess consistency among a larger number of fossils than those preserving all five landmark locations. The subnasal clivus angle marks the orientation in the sagittal plane of the segment nasospinale to prosthion relative to the postcanine alveolar margin, up to the M^2/M^3 septum. It was measured using ImageJ from digital images or CT-based visualizations of a specimen in a lateral

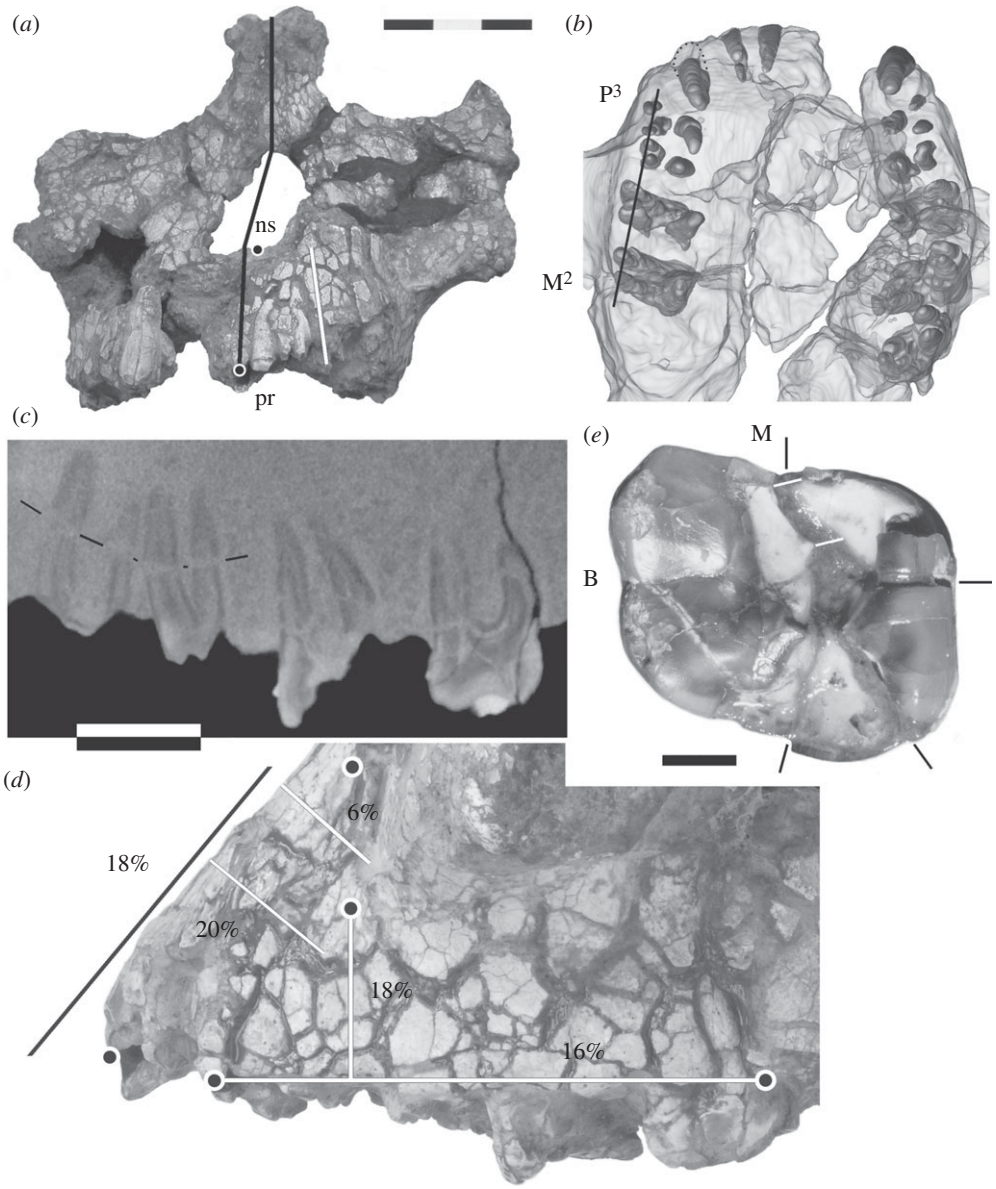

Figure 2. Distortion of KNM-WT 40000. (*a*) Anterior view, giving the midline (black line) to indicate the midface skewing, left nasospinale (ns), prosthion (pr) and the trajectory used to calculate the height expansion of the subnasal area (white line). (*b*) CT-based 3D reconstruction of the maxilla in superior view, showing the tooth roots inside the translucent bone. (*c*) A high-resolution sagittal CT image through the buccal roots of the left P^3 to M^2 (orientation indicated by the black line in (*b*)). The thin black lines mark a longer crack through the premolar roots. (*d*) Lateral view of the left maxilla, showing the pattern of matrix-filled cracks highlighted by wetting with acetone. The five landmarks are shown as in figure 1. The trajectories along which crack widths were measured are given by lines with associated percentages of expansion (black line refers to the subnasal trajectory shown in (*a*)). (*e*) The right M^2 crown (M, mesial; B, buccal), with black lines marking the endpoint of cracks highlighted with acetone. The white lines indicate the match at the mesial end of the widest crack. The dark area on the mesiolingual corner is a strong shadow of the enamel more distally, rather than damage to the dentine. Scale bars, (*a*,*b*) 30 mm, (*c*,*d*) 10 mm and (*e*) 3 mm.

view, where feasible estimating the postcanine alveolar margin orientation if the exact position of landmarks pc or m23 is not preserved. Furthermore, the anterior position of the zygomatic root is considered relative to the dental row, following Lockwood & Tobias (1999, table 7). These features were recorded by the authors from the original specimens, with additional observations regarding zygomatic root position in *A. afarensis* provided by William H. Kimbel (Arizona Sate University, USA).

Finally, the crown size of the right M^2 was assessed on the basis of conventional mesiodistal and buccolingual measurements, defined in two different ways (Tobias 1967; White 1977). Full preparation of the M^2 crown had been done at the time of the first announcement (Leakey *et al.* 2001), and measurements of cracks affecting the length and width had been taken at the time. Comparative data of M^2 size in Plio-Pleistocene hominins were taken from the literature, combined with our own measurements.

3. PRESERVATION OF THE MAXILLA

The facial parts of KNM-WT 40000 show postmortem distortion in the form of lateral skewing of the nasal area and a network of matrix-filled surface

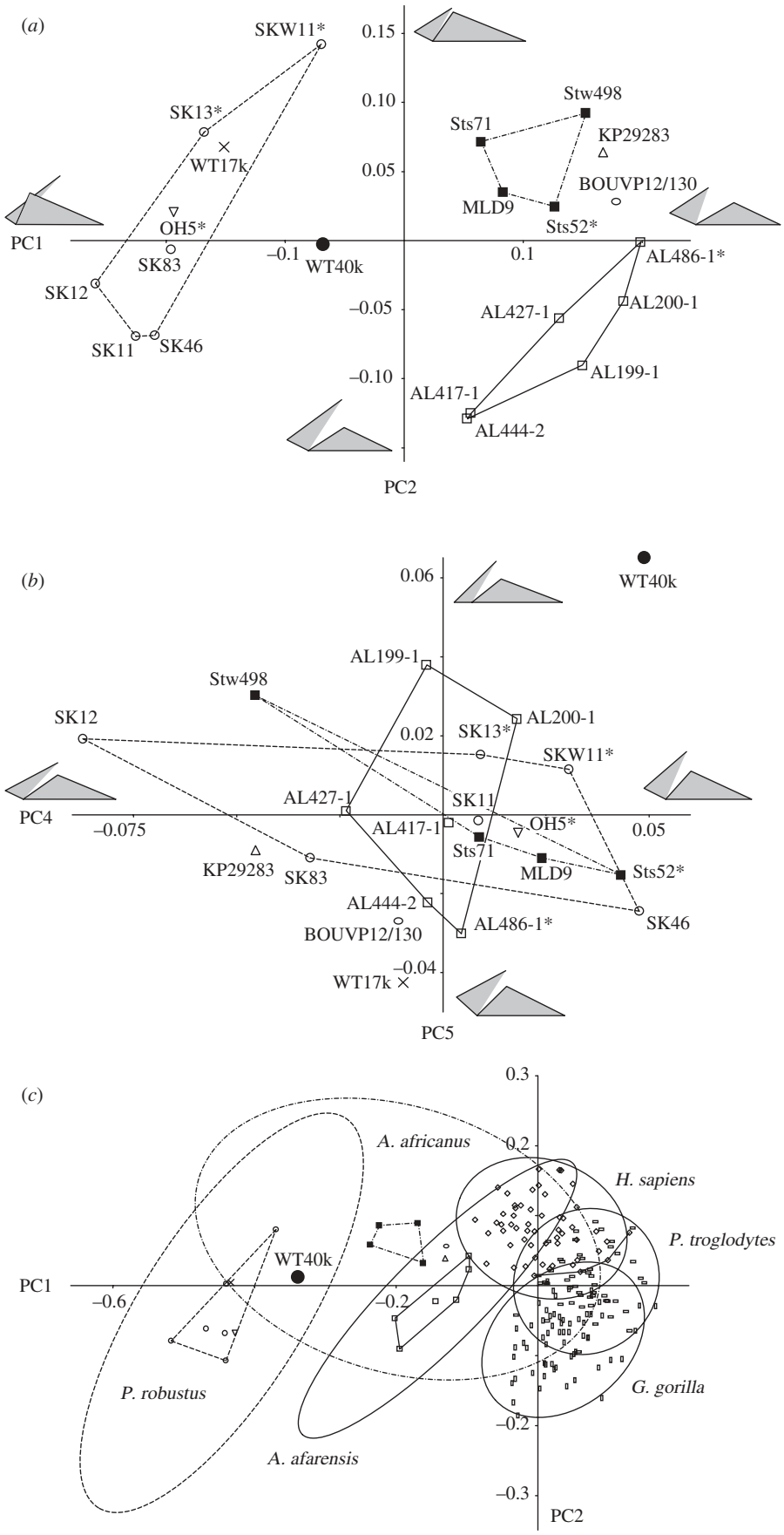

Figure 3. Bivariate plots of PCs. (*a*) PC2 against PC1 and (*b*) PC5 against PC4 of the fossils samples. (*c*) PC2 against PC1 of the combined fossil and extant samples. KNM-WT 40000 (black dot) is corrected for distortion. The prefix KNM- of the Kenyan specimens is omitted, and an asterisk indicates subadults. Convex hulls are given for *A. afarensis* (solid line), *A. africanus* (dash-dot line) and *P. robustus* (dashed line), as well as in (*c*), the 95% confidence ellipses of these taxa and the extant species (solid line). The grey-shaded wire frames in (*a*,*b*) are defined in figure 1 and indicate the maxillary shapes represented at the extremes of the PC axes. See the main text for the percentage of variance represented by each PC.

cracks associated with clay-induced expansion mainly affecting the alveolar and zygomatic processes (Leakey *et al.* 2001; figure 2*a*,*d*). Before assessing the degree of expansion in the landmarked part of the maxilla, it is worth considering whether this area shows any evidence of substantial post-mortem shape changes as well. A good indicator of structural integrity of the alveolar process is the internal preservation of the tooth roots. Those present, of the left I^1 to M^2 and the right C to M^3, are visualized in a CT-based three dimensional reconstruction of the maxilla in superior view (figure 2*b*). The roots are well preserved, without distinct misalignments or distortion, and the dental arcade is symmetrical in shape. The only exception is the largely exposed right canine root which is in the correct position at the alveolar margin, but the apex is tilted anteriorly. A more detailed view of the internal preservation of the left maxilla is provided by a high-resolution sagittal CT image through the buccal roots of the left P^3 to M^2 (figure 2*c*). Several fine cracks through the roots can be seen, and the mesiobuccal root canal of the M^2 is expanded, but this is not accompanied by substantial displacement of the root parts on opposite sides of the cracks. The mesiodistal distance between the P^4, M^1 and M^2 is increased by matrix expansion, particularly of the alveolar space around the roots. However, this is less so between the P^3 and P^4. Overall, the internal CT evidence suggests a pattern of expansion without substantial shape changes due to skewing or other directional deformation. The well-preserved state of the premolar root area is of particular importance as it indicates that the overlying anterior zygomatic process position is unlikely to have been altered by the distortion. This is further confirmed by the absence of major shifts of surface bone fragments between the premolar alveolar margin and the anterior zygomatic root.

The percentages of bone expansion along the measured trajectories vary from 16 per cent along the postcanine alveolar margin to 20 per cent transversely over the canine jugum (figure 2*d*). The one exception is the area superior to the canine alveolus where the expansion in transverse direction is only 6 per cent.

The right M^2 crown is shown in figure 2*e*. The widest crack runs from the mesial interstitial facet to the distolingual corner, a second shorter one from the central area of the main break to the lingual crown margin and a third thin one from the central area to the distal interstitial facet. Enamel and occlusal dentine edges of the breaks provide good clues regarding the match of the four parts they delineate. A refit of the crown would require the two lingual parts to be moved buccally, the triangular distolingual part to be moved mesially and the mesiolingual part to be moved slightly distally. Closing the cracks would result in an estimated 1.2 mm reduction of the buccolingual width of the crown. The mesiodistal length along the crown axis (White 1977) is not affected by the cracks, and has only been corrected for an estimated 0.5 mm of mesial interstitial wear. However, the maximum length (Tobias 1967) requires correction for the 0.7 mm distal displacement of the triangular distolingual part. The buccolingual width is not affected by occlusal wear as it has not reached the level of maximum bulging of the buccal and lingual surfaces. The recently acquired high-resolution CT scans will provide the opportunity to prepare a full three dimensional virtual reconstruction of the right M^2 crown.

4. MORPHOMETRIC COMPARISONS

The PCA of the hominin fossil sample described here uses the corrected landmark configuration of KNM-WT 40000 (table 1). The first six PCs account for 99.9 per cent of the variation. Although PC3–PC6 contribute less than 10 per cent each, these were still assessed because KNM-WT 40000 could specifically differ from the other fossils in morphology that is less variable among the *Australopithecus* and *Paranthropus* specimens which dominate the sample. PC1, PC2, PC4 and PC5 were found to provide evidence in relation to the hypotheses examined here, and these are shown in bivariate plots (figure 3), with wireframes marking the shapes represented at either end of each axis. PC3 and PC6 will be briefly described as well.

PC1 (eigenvalue 0.0263; 72% of variance) represents the variation in anteroposterior position of the anterior zygomatic process (landmark azp) and the relative length and transverse flatness of the subnasal clivus (ns–pr and pr–pc, respectively). PC1 separates *Australopithecus* species, with a more posteriorly positioned zygomatic and a shorter and transversely curved (projecting) subnasal clivus, from *Paranthropus* species, with a more anteriorly positioned zygomatic and a longer and transversely flat subnasal clivus (figure 3*a*). Addressing hypothesis 1, the PC1 score of KNM-WT 40000 differs significantly from that of *A. afarensis* (table 1), reflecting its more anteriorly placed zygomatic and a subnasal clivus that is transversely flat. When compared with multiple species (hypothesis 2), the difference between KNM-WT 40000 and *A. afarensis* is statistically significant, as is the difference from *A. africanus*. The PC1 scores suggest that KNM-WT 40000 is intermediate between *Australopithecus* and *Paranthropus* with respect to this particular morphology. However, the difference from *P. robustus* is not statistically significant, with the subadult SKW 11 having a score close to KNM-WT 40000.

PC2 (eigenvalue 0.0054; 15% of variance) represents both the inferosuperior and anteroposterior position of the zygomatic process and the length of subnasal clivus. This PC separates *A. afarensis*, with a more inferoposteriorly positioned zygomatic and longer subnasal clivus, from *A. africanus*, with a more anterosuperiorly positioned zygomatic and shorter clivus (figure 3*a*). KNM-WT 40000 and *A. garhi* are intermediate, *A. anamensis* falls with *A. africanus*, and *Paranthropus* specimens show the full range of PC2-related morphological variation. KNM-WT 40000 is not significantly different from *A. afarensis* (hypothesis 1) or from other hominin species more in general (hypothesis 2).

PC3 (eigenvalue 0.0029; 8% of variance) purely represents the inferosuperior height of landmark azp, the anterior zygomatic root position, above the postcanine alveolar margin. KNM-WT 40000 does not differ

Table 1. PCs of the maxillary shape analysis. The landmarks of KNM-WT 40000 are corrected for distortion. The sample size (n), mean, minimum, maximum and standard deviation (s.d.) are given, and the comparisons of KNM-WT 40000 by t-test list the probability (p; one-tailed, except $^{+}$two-tailed) and the significance (multiple comparisons after sequential Bonferroni correction). n.s., not significant; $*p < 0.05$; $**p < 0.01$.

		PC1	PC2	PC4	PC5
KNM-WT 40000		−0.068	−0.003	0.049	0.065
A. anamensis	$n = 1$	0.167	0.064	−0.045	−0.009
A. afarensis	n	6	6	6	6
	mean	0.1285	−0.0742	−0.0012	0.0014
	min.	0.053	−0.129	−0.024	−0.030
	max.	0.198	−0.001	0.018	0.038
	s.d.	0.0623	0.0498	0.0136	0.0262
A. garhi	$n = 1$	0.178	0.029	−0.011	−0.027
A. africanus	n	4	4	4	4
	mean	0.1065	0.0558	0.0076	−0.0004
	min.	0.064	0.025	−0.046	−0.015
	max.	0.152	0.092	0.043	0.030
	s.d.	0.0401	0.0316	0.0382	0.0208
P. aethiopicus	$n=1$	−0.152	0.068	−0.010	−0.040
P. robustus	n	6	6	6	6
	mean	−0.1879	0.0073	−0.0040	0.0014
	min.	−0.259	−0.070	−0.087	−0.024
	max.	−0.070	0.142	0.048	0.019
	s.d.	0.0654	0.0855	0.0488	0.0169
P. boisei	$n = 1$	−0.194	0.020	0.018	−0.005
comparison with *A. afarensis*					
	p	0.016	0.120	0.010	0.037
	sign.	*	n.s.	**	*
comparison with *Australopithecus* and *Paranthropus*					
A. afarensis	p	0.016	0.120	0.010	0.037
	sign.	*	n.s.	*	*
A. africanus	p	0.015	0.098	0.204	0.034
	sign.	*	n.s.	n.s.	n.s.
P. robustus	p	0.151^{+}	0.919^{+}	0.182	0.009
	sign.	n.s.	n.s.	n.s.	*

significantly from *A. afarensis*, *A. africanus* or *P. robustus*, and this morphology does not relate to the hypotheses.

PC4 (eigenvalue 0.0011; 3% of variance) represents the subnasal clivus orientation associated with variations in the midline area only, as shown by the angle of ns–pr to the entire alveolar margin (pr–pc–m23; figure 3*b*). KNM-WT 40000 has the highest score in the sample and is significantly less prognathic than *A. afarensis* (table 1). When compared with multiple species, this difference from *A. afarensis* is statistically significant as well, but differences from *A. africanus* and *P. robustus* are not.

PC5 (eigenvalue 0.0006; 2% of variance) represents the subnasal clivus orientation associated with variations of the entire subnasal area. The midline clivus (ns–pr) and the canine–incisor alveolar margin (pr–pc) jointly vary in orientation relative to the postcanine alveolar margin (pc–m23; figure 3*b*). KNM-WT 40000 is by far the most orthognathic in the sample, and the difference from *A. afarensis* is statistically significant (table 1, figure 3*b*). When compared with multiple species, KNM-WT 40000 is significantly different from *A. afarensis* and *P. robustus*.

PC4 and PC5 jointly contribute to an overall pattern of differences in subnasal prognathism in the fossil sample (figure 3*b*). KNM-WT 40000 is the most orthognathic, whereas the *P. aethiopicus* specimen KNM-WT 17000, the *A. garhi* type BOU-VP-12/130 and the *A. anamensis* specimen KNM-KP 29283 are the most prognathic. The other species of *Australopithecus* and *Paranthropus* do not differ notably.

PC6 (eigenvalue 0.0003; 1% of variance) represents the angle and length proportions between the alveolar margins of the anterior (canine–incisor) and postcanine teeth. There is no separation between taxa, and KNM-WT 40000 does not differ significantly from *A. afarensis*, *A. africanus* and *P. robustus*.

Using the landmark configuration of KNM-WT 40000 as preserved rather than corrected for distortion results in PC scores that are only marginally different from those reported in table 1. Significance levels of the t-tests are the same as for the corrected landmarks, except for multiple species comparisons of PC5 with *A. afarensis* and *A africanus* (electronic supplementary material, S1). When excluding the five subadult specimens from the fossil samples, KNM-WT 40000 differs significantly from *A. afarensis* for PC1, 4 and 5, as

Table 2. Mahalanobis' distance test comparing KNM-WT 40000 using all PCs combined. D^2, squared Mahalanobis' distance of KNM-WT 40000 from centroid of species sample; SDU, standard deviation unit of Mahalanobis' distances within the sample; d.f., degrees of freedom; *p*, probability that KNM-WT 40000 belongs to the species. For sample sizes less than six, the probability is not calculated (n/a) because estimates of the variance are insufficiently reliable.

	D^2	SDU	d.f.	*p*-value
KNM-WT 40000 (corrected)				
A. afarensis	21.065	4.589	6	<0.0025
A. africanus	37.084	6.089	4	n/a
P. robustus	13.284	3.644	6	<0.05
KNM-WT 40000 (as preserved)				
A. afarensis	18.909	4.348	6	<0.005
A. africanus	36.609	6.050	4	n/a
P. robustus	13.738	3.706	6	<0.05
KNM-WT 40000 (corrected), adults only				
A. afarensis	33.088	5.752	5	n/a
A. africanus	28.397	5.328	3	n/a
P. robustus	20.390	4.515	4	n/a

Table 3. Interspecific comparisons of the standard deviations of PC1 and PC2 obtained in the maxillary shape analysis, giving *F* and probability (*p*) values. The differences are not statistically significant after sequential Bonferroni correction.

	PC1		PC2	
	F	*p*-value	*F*	*p*-value
A. afarensis–H. sapiens	1.010	0.865	1.441	0.450
A. afarensis–P. troglodytes	1.083	0.758	1.192	0.648
A. afarensis–G. gorilla	1.371	0.503	1.368	0.505
A. africanus–H. sapiens	1.570	0.811	2.233	0.560
A. africanus–P. troglodytes	1.435	0.885	2.698	0.451
A. africanus–G. gorilla	1.134	0.914	2.351	0.529
P. robustus–H. sapiens	1.023	0.827	2.954	0.040
P. robustus–P. troglodytes	1.119	0.720	2.445	0.088
P. robustus–G. gorilla	1.416	0.470	2.805	0.053

before, but for PC2 as well (electronic supplementary material, S2). When compared with multiple species, KNM-WT 40000 differs significantly from *A. afarensis* for PC4 and from *P. robustus* for PC1.

Results of Mahalanobis' distance tests comparing KNM-WT 40000 with *A. afarensis*, *A. africanus* and *P. robustus* individually, and using all PCs combined, are given in table 2. Differences from *A. afarensis* and *P. robustus* are statistically significant, whereas the *A. africanus* sample is too small for a probability to be calculated.

A PCA of the fossil hominins combined with modern humans, chimpanzees and gorillas shows how the main aspects of variation of the fossil samples, as reflected by PC1 and PC2 (48% and 19% of the variance), compare with those shown by larger samples of extant species. A bivariate plot of PC2 against PC1 shows that the areas of observed variation (convex hulls) of *A. afarensis* and *P. robustus* are not substantially different from those of the extant species, whereas *A. africanus*, with fewer specimens in the sample, appears somewhat less variable (figure 3*c*). With samples sizes of 50 or more, 95% confidence ellipses of the extant species have a close fit with the observed variation, but for the small fossil samples the ellipses are large. Importantly, *F*-tests indicate that the standard deviations of PC1 and PC2 obtained for the fossil taxa are not significantly different from those of the extant species (table 3).

The M^2 crown size of KNM-WT 40000 falls below the currently known range of variation of all hominin species included in the comparisons (table 4). Its mesiodistal length is the same as the minimum known for *A. anamensis*, but the particular specimen has a larger buccolingual width than KNM-WT 40000 (KNM-ER 30200: 13.2 as opposed to 12.4). Statistically, both the mesiodistal length and buccolingual width are significantly smaller in KNM-WT 40000 than in *A. afarensis* (table 4). When compared with multiple species of *Australopithecus* and *Paranthropus*, its mesiodistal length is only significantly smaller than in *P. boisei*, but its buccolingual width is smaller than in all species other than *A. anamensis*.

5. DISCUSSION

The taxonomic diagnosis of *K. platyops* and initial description of its type specimen KNM-WT 40000 were mainly based on qualitative comparisons (Leakey *et al.* 2001). Here we analyse the maxilla of KNM-WT 40000 quantitatively and test the specific hypotheses that the specimen is not different from the contemporary taxon *A. afarensis* and, more broadly, that it is not different from species of *Australopithecus* and *Paranthropus*. Based on the analyses of maxillary shape and M^2 crown size, both hypotheses can be rejected. These findings thus support the notion that there was hominin species diversity in the Middle Pleistocene and corroborate the validity of *K. platyops* as a separate species. It is worth pointing out that the observed differences are substantial, given that statistical significance is obtained for small samples, with Bonferroni corrections when comparing KNM-WT 40000 with multiple species. Moreover, comparisons of the *A. afarensis*, *A. africanus* and *P. robustus* samples used here with larger samples of modern humans, chimpanzees and gorillas indicate that these fossils show representative levels of intraspecific morphological variation. Hence, the observed differences from KNM-WT 40000 are unlikely to be an artefact of under-sampled variation in the three fossil species.

The observation by Leakey *et al.* (2001) that the M^2 crown size of KNM-WT 40000 is smaller than the known range of variation shown by species of *Australopithecus* and *Paranthropus* is upheld here based on the largest sample currently available. The difference is most distinct for the buccolingual width. This is the more reliable measure in KNM-WT 40000 as it is not affected by interstitial or occlusal wear, and the crack expanding the width is well defined and can be corrected for with confidence.

Table 4. Mesiodistal (MD) length and buccolingual (BL) width of the M^2, and the subnasal clivus (ns-pr) angle to the postcanine alveolar margin. The sample size (*n*), mean, minimum, maximum and standard deviation (s.d.) are given. Comparisons by *t*-test of KNM-WT 40000 with hominin species list the probability (*p*, one-tailed) and significance (n.s., not significant; multiple comparisons with sequential Bonferroni correction). MD1 and BL1 defined after White (1977), MD2 and BL2 after Tobias (1967). The subnasal clivus angle was measured among adult and subadult specimens (M^2 in full occlusion) listed in the electronic supplementary material, S3. $*p < 0.05$; $**p < 0.01$; $***p < 0.001$.

		M^2 size					subnasal angle
		MD1	MD2	BL1	BL2	source	
KNM-WT 40000		11.4	11.9	12.4	12.8	Leakey *et al.* (2001), this study	47
A. anamensis	*n*	8	—	8	—	Ward *et al.* (2001), White *et al.* (2000)	1
	mean	12.88		14.50			27
	min.	11.4		12.9			
	max.	14.3		16.7			
	s.d.	1.04		1.19			
A. afarensis	*n*	12	—	13	—	Kimbel & Delezene (2009)	6
	mean	13.00		14.80			34.6
	min.	12.1		13.4			29
	max.	14.1		15.8			39
	s.d.	0.60		0.60			3.5
A garhi	$n = 1$	14.4	—	17.7	—	Asfaw *et al.* (1999)	27
A. africanus	*n*	—	24	—	28	Moggi-Cecchi *et al.* (2006), J. Moggi-Cecchi	9
	mean		14.12		15.95	(2006, personal communication), this study	34.2
	min.		12.6		13.5		30
	max.		16.6		17.9		37
	s.d.		1.09		1.23		1.9
P. aethiopicus	$n = 1$	—	—	—	—		31
P. robustus	*n*	—	24	—	24	J. Moggi-Cecchi (2006, personal communication),	8
	mean		14.00		15.73	this study	36.8
	min.		11.6		14.0		32
	max.		15.7		16.9		39
	s.d.		0.99		0.94		4.1
P. boisei	*n*	—	6	—	6	Tobias (1967), Leakey & Walker (1988), Wood	2
	mean		15.84		18.18	(1991), this study	35.9
	min.		14.7		16.6		33
	max.		17.2		21.0		39
	s.d.		1.03		1.55		
comparison with *A. afarensis*							
	p	0.013		0.001			0.011
	sign.	*		**			*
comparison with *Australopithecus* and *Paranthropus*							
A. anamensis	*p*	0.111		0.073			
	sign.	n.s.		n.s.			
A. afarensis	*p*	0.013		0.001			0.011
	sign.	n.s.		**			*
A. africanus	*p*		0.029		0.010		0.000
	sign.		n.s.		*		***
P. robustus	*p*		0.024		0.003		0.024
	sign.		n.s.		*		*
P. boisei	*p*		0.008		0.012		
	sign.		*		*		

The geometric morphometric shape analysis of the maxilla shows that zygomatic process position together with subnasal clivus length and transverse flatness account for most of the variance in the hominin fossil sample (PC1 and PC2 combined, 86%, figure 3*a*). PC1 associates a more anteriorly positioned zygomatic process with a transversely flatter and longer subnasal clivus, along a gradient of genera: *Paranthropus*, *Kenyanthropus* (i.e. KNM-WT 40000) and *Australopithecus*. In contrast, PC2 associates a more anteriorly positioned zygomatic process with a shorter subnasal clivus and separates *A. afarensis* from *A. africanus* only. There is no evidence of intraspecific differences within *Paranthropus* regarding PC1 and PC2, as KNM-WT 17000 and OH 5 fall in the middle of the range of *P. robustus*.

Apart from zygomatic root position and transverse subnasal flatness, subnasal prognathism is a third

Table 5. Anterior position of the zygomatic process along the dental row. Accession codes CH, ER, KP and WT lack the prefix KNM-.

	P^3	P^3/P^4	P^4	P^4/M^1	M^1
A. anamensis			KP 29283		
A. afarensis			A.L. 442-1	A.L. 58-22	A.L. 199-1
				A.L. 200-1a	A.L. 333-2
				A.L. 333-1	A.L. 413-1
				A.L. 427-1	A.L. 417-1d
				A.L. 444-2	A.L. 822-1
				A.L. 486-1[a]	
				A.L. 651-1	
A. garhi				BOU-VP-12/130	
A. africanus		Sts 52[a]	MLD 6	MLD 9	Sts 5
			MLD 45	TM 1511	
			Sts 17	TM 1512	
			Sts 52[a]	TM 1514	
			Sts 53	Sts 63	
			Sts 71	Sts 3009	
			Stw	Stw 13	
			252[a,b]	Stw	
			Stw 391	183[a,b]	
			Stw 505	Stw 498	
K. platyops		WT 40000			
		WT 38350			
P. aethiopicus		WT 17000			
P. robustus	SK 13[a]	TM 1517	DNH 7		
	SK 47[a]	SK 48	SK 11		
	SK 821	SK 52[a]	SK 12		
		SK 79	SK 29		
		SK 83	SK 46		
		SKW 11[a]	SK 79		
			SKW 12		
P. boisei	KGA 10-525	KGA 10-525			
	CH 1B[a]	ER 405			
	ER 732	ER 406			
	WT 17400[a]	OH 5			

[a]Immature specimen.
[b]Listed as *A. africanus*, but affinities uncertain (Lockwood & Tobias 2002).

prominent aspect of maxillary shape characterizing KNM-WT 40000. It is also expressed by two separate patterns of variation (PC4 and PC5; figure 3*b*), which differ depending on whether the clivus orientation varies in the midline only (PC4), or involves the entire subnasal area, from canine jugum to canine jugum bilaterally (PC5). As most specimens in the sample (*P. robustus*, *P. boisei*, *A. afarensis* and *A. africanus*) tend to show similar levels of prognathism, this morphology does account for only 5 per cent of the variance in the total sample. However, it does single out the orthognathic morphology of KNM-WT 40000 and to a lesser extent the more prognathic shape in *A. anamensis*, *A. garhi* and *P. aethiopicus*. This pattern illustrates that in interspecific comparisons the higher PCs associated with small amounts of overall variance can provide highly relevant information regarding individual specimens, because the distribution of the variance depends on the sample composition.

In all, the analyses confirm the occurrence of three different facial patterns among the early hominins considered here. *Australopithecus* is characterized by a prognathic, transversely curved subnasal area combined with posteriorly positioned zygomatics (figure 1*a*), *Paranthropus* by a prognathic, transversely flat subnasal area with anteriorly positioned zygomatics and *Kenyanthropus* by a more orthognatic, transversely flat subnasal area with anteriorly positioned zygomatics (figure 1*b*).

Two of the facial features, the degree of midline subnasal prognathism and the position of the zygomatic process, can be quantified individually in a larger number of early hominin specimens than could be included in the geometric morphometric analyses. It can thus be assessed whether the evidence from larger samples is consistent with the landmark-based results. The subnasal angle, which combines the shape variation associated with PC4 and PC5, is larger in KNM-WT 40000 (47°) than in any of the *Australopithecus* and *Paranthropus* specimens that could be measured (27–39°; table 4, electronic supplementary material, S3). Those differences that can be tested, from *A. afarensis*, *A. africanus* and *P. robustus*, are statistically significant. The anterior zygomatic root positions of early hominins, associated with PC1 and PC2, are summarized in table 5. The position in KNM-WT 40000 at the level of the P^3/P^4 interalveolar septum is commonly found in *Paranthropus* as well. On the other hand, it falls outside the range of variation of *Australopithecus*, with the

exception of the left side of the subadult specimen Sts 52. Importantly, in *A. afarensis*, the position is always more posterior, in one instance at the distal half of P^4, and more commonly at the P^4/M^1 septum or M^1. Hence, these univariate observations do fully confirm the characterization of *K. platyops* as subnasally orthognathic combined with anteriorly positioned zygomatics.

The *A. afarensis* specimen most similar in geological age to KNM-WT 40000 is the Garusi 1 maxilla (Laetoli approx. 3.6 Ma). It is too fragmentary to be included in the PCA, or even to allow the quantification of subnasal clivus orientation or zygomatic process position. However, it is possible to make some inferences about its morphology that are relevant here. There is no evidence of the zygomatic root in the premolar area, and the anterior position must thus have been at P^4/M^1 or more posteriorly. Subnasally, Garusi 1 is very prognathic, has rounded nasal margins around the canine alveoli and lacks a clear nasal sill. In the latter characters, it differs from the *A. afarensis* Hadar sample and is more similar to *A. anamensis* (Kimbel *et al.* 2006; Kimbel 2007), and in all these aspects, Garusi 1 contrasts strongly with KNM-WT 40000.

KNM-WT 40000 is poorly preserved, and Leakey *et al.* (2001) reported on the specimen by extracting meaningful information from selected areas after carefully mapping the post-mortem distortion. Bone expansion associated with clay-filled cracks is frequently encountered among fossils found in the Turkana Basin and has been routinely recognized as a phenomenon affecting a specimen's morphology (e.g. the descriptions in Wood 1991). Naming it expanding matrix distortion, White (2003) states to have 'formalized' this taphonomic process, defining five stages. He assigned KNM-WT 40000 to stage 4, but as no definition of these stages has been published, it is not possible to evaluate this classification. It is worth pointing out that some areas of the cranium, such as parts of the left temporal bone, show very little distortion, whereas others, such as the cranial vault, are highly affected. Thus, characterizing the specimen by a single stage has little value.

The analyses presented here show that the distortion has had little impact on the characters of maxillary shape relevant to the diagnosis of *K. platyops*. The preservation of the tooth roots and the integrity of the dental arcade indicate that distinct directional shape changes, such as skewing or compression, did not occur in the lower part of the left maxilla. Expansion cracks did cause a size increase of about 18 per cent, but this occurred mostly at a similar rate across the area, thus having little effect on shape. In all, there is no indication that the position of the zygomatic root or the subnasal clivus shape were modified substantially, particularly in a way that would mimic normal morphological differences between species. The only striking contrast in expansion rate was found between the area above (6%) and over the left canine jugum (20%). This difference is consistent with the CT-based observation that internal expansion is strongest in the alveolar space around the roots, a phenomenon that is understandable as it becomes readily filled with clay, unlike trabecular bone not open to the outside. Moreover, positioned at the corner of the dental arcade, the canine alveolus has more thin overlying bone than other teeth, making the jugum particularly vulnerable to cracking.

Apart from the zygomatic process position, subnasal clivus morphology and a small upper molar size Leakey *et al.* (2001) also lists similarly sized I^1 and I^2 roots and upper premolars that are three-rooted as features characterizing the maxilla of *K. platyops*. These have not been considered here, but warrant further study. The unusual incisor root proportions (figure 2*b*) and their spatial relationship to the transversely flat, orthognathic subnasal area is of particular interest, and using high-resolution CT this can now be examined in more detail.

The partial maxilla KNM-WT 38350 shares with KNM-WT 40000 the anterior zygomatic root position, three-rooted premolars and a small molar size and was therefore designated as the paratype of *K. platyops* (Leakey *et al.* 2001). However, it is too fragmentary a specimen to enable a full comparison with the unique facial morphology of KNM-WT 40000. The partial mandible KT12/H1, the holotype of the broadly contemporary species *A. bahrelghazali*, is characterized by a sagittally and transversely flat anterior corpus, said to reflect a more orthognathic face (Brunet *et al.* 1996). If correct, this would increase the likelihood that KNM-WT 40000 and KT12/H1 are conspecific. However, the association between subnasal and symphyseal shapes is not well understood (Spoor *et al.* 2005), and how *K. platyops* relates to *A. bahrelghazali* remains unclear. Thus, although there is good evidence, presented here and elsewhere (Leakey *et al.* 2001; Guy *et al.* 2008), of hominin species diversity in the Middle Pliocene of Africa, additional fossils will be required to reveal the full nature and interrelationships of the lineages present at that time.

We thank Alan Walker and Chris Stringer for inviting us to contribute this work and the National Museums of Kenya, the National Museum of Ethiopia, the Transvaal Museum (South Africa), Department of Anatomy, Witwatersrand University (South Africa), the Institute of Human Origins (USA) and the museums listed in §2 for access to specimens in their care. We are grateful to Berhane Asfaw, Michel Brunet, Ron Clarke, Nick Conard, Chris Dean, Heidi Fouri, Philipp Gunz, John Harrison, Jean Jacques Hublin, Louise Humphrey, Paula Jenkins, Don Johanson, Andre Keyser, Bill Kimbel, Rob Kruszynski, Kornelius Kupczik, the late Charlie Lockwood, Emma Mbua, Jacopo Moggi-Cecchi, Sam Muteti, Paul O'Higgins, Matt Skinner, Gen Suwa, Heiko Temming, Brian Villmoare, Tim White and Andreas Winzer for help with various aspects of this study. Financial support was provided by the Leakey Foundation, the National Geographic Society and the Max Planck Society.

REFERENCES

Asfaw, B., White, T., Lovejoy, O., Latimer, B., Simpson, S. & Suwa, G. 1999 *Australopithecus garhi*: a new species of early hominid from Ethiopia. *Science* **284**, 629–635. (doi:10.1126/science.284.5414.629)

Boaz, N. T. 1988 Status of *Australopithecus afarensis*. *Yrbk. Phys. Anthropol.* **31**, 85–113. (doi:10.1002/ajpa.1330310506)

Brown, B., Brown, F. & Walker, A. 2001 A. New hominids from the Lake Turkana Basin, Kenya. *J. Hum. Evol.* **41**, 29–44. (doi:10.1006/jhev.2001.0476)

Brunet, M., Beauvillain, A., Coppens, Y., Heintz, E., Moutaye, A. H. E. & Pilbeam, D. 1995 The first australopithecine 2 500 kilometres west of the Rift Valley (Chad). *Nature* **378**, 273–274. (doi:10.1038/378273a0)

Brunet, M., Beauvillain, A., Coppens, Y., Heintz, E., Moutaye, A. H. E. & Pilbeam, D. 1996 *Australopithecus bahrelghazali*, une nouvelle espèce d'hominidé ancien de la région de Koro Toro (Tchad). *C. R. Acad. Sci. Paris* **322**, 907–913.

Cobb, S. 2008 The facial skeleton of the chimpanzee–human last common ancestor. *J. Anat.* **212**, 469–485. (doi:10.1111/j.1469-7580.2008.00866.x)

Guy, F., Mackaye, H. T., Likius, A., Vignaud, P., Schmittbuhl, M. & Brunet, M. 2008 Symphyseal shape variation in extant and fossil hominoids, and the symphysis of *Australopithecus bahrelghazali*. *J. Hum. Evol.* **55**, 37–47. (doi:10.1016/j.jhevol.2007.12.003)

Hammer, Ø., Harper, D. A. T. & Ryan, P. D. 2001 PAST: paleontological statistics software package for education and data analysis. *Palaeontol. Electron.* **4**, 1–9.

Kimbel, W. K. 2007 The species and diversity of australopiths. In *Handbook of Paleoanthropology*, vol. III (eds W. Henke, T. Hardt & I. Tattersall), pp. 1539–1573. Berlin, Germany: Springer.

Kimbel, W. H. & Delezene, L. K. 2009 'Lucy' redux: a review of research on *Australopithecus afarensis*. *Yrbk. Phys. Anthropol.* **52**, 2–48. (doi:10.1002/ajpa.21183)

Kimbel, W. H., Rak, Y. & Johanson, D. C. 2004 *The skull of Australopithecus afarensis*. New York, NY: Oxford University Press.

Kimbel, W. H., Lockwood, C. A., Ward, C. V., Leakey, M. G., Rak, Y. & Johanson, D. C. 2006 Was *Australopithecus anamensis* ancestral to *A. afarensis*? A case of anagenesis in the early hominin fossil record. *J. Hum. Evol.* **51**, 134–152. (doi:10.1016/j.jhevol.2006.02.003)

Leakey, R. E. F. & Walker, A. 1988 New *Australopithecus boisei* specimens from East and West Lake Turkana, Kenya. *Am. J. Phys. Anthropol.* **76**, 1–24. (doi:10.1002/ajpa.1330760102)

Leakey, M. G., Spoor, F., Brown, F. H., Gathogo, P. N., Kiarie, C., Leakey, L. N. & McDougall, I. 2001 New hominin genus from eastern Africa shows diverse middle Pliocene lineages. *Nature* **410**, 433–440. (doi:10.1038/35068500)

Lockwood, C. A. & Tobias, P. V. 1999 A large male hominin cranium from Sterkfontein, South Africa, and the status of *Australopithecus africanus*. *J. Hum. Evol.* **36**, 637–685. (doi:10.1006/jhev.1999.0299)

Lockwood, C. A. & Tobias, P. V. 2002 Morphology and affinities of new hominin cranial remains from Member 4 of the Sterkfontein Formation, Gauteng Province, South Africa. *J. Hum. Evol.* **42**, 389–450. (doi:10.1006/jhev.2001.0532)

Lockwood, C. A., Richmond, B. G., Jungers, W. L. & Kimbel, W. H. 1996 Randomization procedures and sexual dimorphism in *Australopithecus afarensis*. *J. Hum. Evol.* **31**, 537–548. (doi:10.1006/jhev.1996.0078)

Lockwood, C. A., Kimbel, W. H. & Johanson, D. C. 2000 Temporal trends and metric variation in the mandibles and dentition of *Australopithecus afarensis*. *J. Hum. Evol.* **39**, 23–55. (doi:10.1006/jhev.2000.0401)

Moggi-Cecchi, J., Grine, F. E. & Tobias, P. V. 2006 Early hominid dental remains from Members 4 and 5 of the Sterkfontein Formation (1966–1996 excavations): catalogue, individual associations, morphological descriptions and initial metrical analysis. *J. Hum. Evol.* **50**, 239–328. (doi:10.1016/j.jhevol.2005.08.012)

Nevell, L. & Wood, B. 2008 Cranial base evolution within the hominin clade. *J. Anat.* **212**, 455–468. (doi:10.1111/j.1469-7580.2008.00875.x)

O'Higgins, P. & Jones, N. 1998 Facial growth in *Cercocebus torquatus*: an application of three dimensional geometric morphometric techniques to the study of morphological variation. *J. Anat.* **193**, 251–272. (doi:10.1046/j.1469-7580.1998.19320251.x)

Rice, W. R. 1989 Analyzing tables of statistical tests. *Evolution* **43**, 223–225. (doi:10.2307/2409177)

Spoor, F., Leakey, M. G. & Leakey, L. N. 2005 Correlation of cranial and mandibular prognathism in extant and fossil hominids. *Trans. R. Soc. S. Afr.* **60**, 85–89.

Strait, D. S. & Grine, F. E. 2004 Inferring hominoid and early hominid phylogeny using craniodental characters: the role of fossil taxa. *J. Hum. Evol.* **47**, 399–452. (doi:10.1016/j.jhevol.2004.08.008)

Tobias, P. V. 1967 *The cranium and maxillary dentition of Australopithecus (Zinjanthropus) boisei. Olduvai Gorge*, vol. 2. Cambridge, UK: Cambridge University Press.

Ward, C. V., Leakey, M. G. & Walker, A. 2001 Morphology of *Australopithecus anamensis* from Kanapoi and Allia Bay, Kenya. *J. Hum. Evol.* **41**, 255–368. (doi:10.1006/jhev.2001.0507)

White, T. D. 1977 New fossil hominids from Laetolil, Tanzania. *Am. J. Phys. Anthropol.* **46**, 197–230. (doi:10.1002/ajpa.1330460203)

White, T. D. 2003 Early hominids—diversity or distortion? *Science* **299**, 1994–1997. (doi:10.1126/science.1078294)

White, T. D., Suwa, G., Simpson, S. & Asfaw, B. 2000 Jaws and teeth of *Australopithecus afarensis* from Maka, Middle Awash, Ethiopia. *Am. J. Phys. Anthropol.* **111**, 45–68. (doi:10.1002/(SICI)1096-8644(200001)111:1<45::AID-AJPA4>3.0.CO;2-I)

Wood, B. 1991 *Koobi Fora research project. Vol. 4: hominid cranial remains*. Oxford, UK: Clarendon Press.

Wood, B. & Lonergan, N. 2008 The hominin fossil record: taxa, grades and clades. *J. Anat.* **212**, 354–376. (doi:10.1111/j.1469-7580.2008.00871.x)